

# A Forecasting Model Based on Time Series Analysis Applied to Electrical Energy Consumption

Carmine Tepedino, Claudio Guarnaccia, Svetoslav Iliev, Silviya Popova and Joseph Quartieri

**Abstract**—One of the main objectives of the European Union (EU) is the reduction of energy consumption and the elimination of energy wastage. These two issues are extremely important, especially in large energy demanding areas, such as transportation, manufacturing, etc.. Electricity consumption prediction is a basic tool for energy management system. Precise prediction of transportation companies helps the energy providers to make right decision for proper distribution of electricity. In this paper, the authors present a Time Series Analysis Model and its application to the electricity consumption of public transportation in Sofia (Bulgaria) in 2011, 2012 and 2013. This technique is based on the dataset analysis and is able to arise the trend slope, the periodic pattern and the random component as a function of time. The innovation of the presented model is in the multiple seasonality and in its ability in following the monthly oscillations. The dataset analysed will show a strongly periodic pattern that will be reconstructed with three different seasonal coefficients. The adoption of statistical tests for linearity and stationarity will show that the series under study is nonlinear and stationary. Comparison between models with two and three seasonalities will be performed in terms of error analysis. A validation on the January 2013 dataset for the triple seasonality model will show interesting results in terms of very low mean error and standard deviation. In addition, a proper interpretation of the model coefficients will open the way to the implementation of improved energy management strategies.

**Keywords**—Electricity consumption, Time Series, Multiple seasonality, Error analysis.

## I. INTRODUCTION

**N**OWADAYS efficient energy management is extremely important in large cities. There are several benefits that can derive from an accurate description and forecasting of electricity consumption. The first one relates to the management of the energy system of the city. The energy provider requires each large consumer to declare in advance the energy needed for a given period of time. Another benefit is economic. The cost of exceeding energy, i.e. the energy

consumed above a stated amount, is much higher than the primary one. For instance, transportation companies has to declare the predicted consumption in a certain time range and, if the consumption is higher than the declared one, the missing energy is bought at double price, while, if the need is lower, the excess energy is sold at lower prices, with consequent economic losses. An additional benefit of predictive model is the opportunity to develop various business strategies, based on the forecasted energy consumptions in different routes and number of vehicles scenarios, with the aim of reducing the energy demand and to offer an adequate service.

It is important to highlight that in many advanced countries, in order to improve energy management in the electrical grid, some relevant energy consumers have the possibility to split their loads in a continuously necessary part and in a detachable part. In the transportation case, for instance, the electrical engine of buses requires continuous energy availability, but the electrical energy used for heating systems is a detachable load. If the bus company knows the correct amount of the two load types and can forecast the two types of absorption, it can participate on a smart grid in a Demand Response Resource (DRR) system [1, 2]. Demand response programs are being used by electric system planners and operators as resource options for balancing supply and demand. Demand response provides an opportunity for consumers to play a significant role in the operation of the electric grid by reducing or shifting their electricity usage during peak periods in response to time-based rates or other forms of financial incentives [3].

DRRs are demand-side entities which actively participate in the markets as both buyers of electricity and sellers of load curtailment services. The objective of demand response is to make the load an active participant in balancing electricity supply and demand around the clock via side-by-side competition with supply-side resources. DRRs curtail their loads in response to incentive payments to lower electricity consumption at specified times. For this reasons, a reliable prediction can be extremely useful to design and perform DRRs.

In general, several advanced predictive models are present in literature, based on different approaches such as Neural Networks, Support Vector Machines, Fuzzy logic, statistical tools, Cellular Automata, some of them applied to energy consumption (see for instance [4-15]).

C. Guarnaccia, J. Quartieri and C. Tepedino, are with the Department of Industrial Engineering, University of Salerno, Via Giovanni Paolo II, I-84084 Fisciano (SA) – ITALY (corresponding: [cguarnaccia@unisa.it](mailto:cguarnaccia@unisa.it) , [quartieri@unisa.it](mailto:quartieri@unisa.it) , [ctepedino@unisa.it](mailto:ctepedino@unisa.it) ).

S. Popova and S. Iliev are with the Department of Bioengineering, Institute of Systems Engineering and Robotics - Bulgarian Academy of Sciences - Sofia 1113, Akad. G. Bonchev str.,bl BULGARIA (Popova\_Silvia2000@yahoo.com, [sd\\_iliev@abv.bg](mailto:sd_iliev@abv.bg)).

Time Series Analysis (TSA) models are able to consider the trend, the periodic and the random components of a certain set of data varying over the time. They have been adopted for the prediction of road traffic noise [16, 17] and the comparison with other traffic noise models ([18-30]) showed good performances, both in the case of single seasonal coefficient and in the case of double periodicity. Another application of TSA model can be the prediction of air pollution components time evolution. For instance, in [31] the hourly CO concentration in Monterrey area (Mexico) is modelled by means of a TSA model. In this case, the general trend was achieved, while the local oscillations were roughly predicted. In this paper a multiple seasonality TSA model is presented and applied to the electricity consumption of local transportation in Sofia (Bulgaria). The goal is to obtain an adequate model describing the process, to be used to predict the electricity required for a given future period.

## II. METHODS

### A. Model presentation

The Time Series Analysis (TSA) model adopted in this paper is largely used in several domains, such as Economics, Physics, Engineering, Mathematics, etc. (see for instance [32-36]). In particular, the authors applied these techniques to road traffic noise prediction [16, 17] and to air pollution [31], obtaining good predicting performances.

The general idea of these TSA models is to reproduce the behavior of the data and to predict the future slope, by composing the trend and the periodicity of the time series, and by adding an error component obtained analyzing the residuals in the calibration phase. The latter component is in charge of compensating the oscillations due to the random part of the time series (background noise). The way these three parts are composed define a multiplicative, additive or mixed model.

The detailed description of the TSA model procedure, with single seasonality pattern, can be found in [16]. The formula of the forecast  $F_t$  is:

$$F_t = T_t \bar{S}_i \quad (1)$$

where  $T_t$  is the trend,  $\bar{S}_i$  is the seasonal coefficient.

The trend is calculated as a linear regression on the observed data.

It is important to underline that the more significant is the periodicity of the time series, the more precise will be the model prediction. When two periodicities are present in the data (such as in [17]), it is necessary to use two seasonal coefficients. The forecast formula of the Double Seasonality TSA model (DSM) is:

$$F_t = T_t \bar{S}_{1,i} \bar{S}_{2,j} \quad (2)$$

where  $\bar{S}_{1,i}$  and  $\bar{S}_{2,j}$  are the two different coefficients.

In order to remove the effects of short period seasonality from the data, a centred moving average with width  $k_1$  (first

lag detected) can be used. Then, it is possible to evaluate the recurring effect,  $S_{1,t}$ , on the single hour by the ratio between the actual data at time  $t$  and the centred moving average at the same  $t$ :

$$S_{1,t} = \frac{A_t}{M_{(k_1)t}} \quad (3)$$

Where  $A_t$  is the actual value and  $M_{(k_1)t}$  is the centred moving average with width  $k_1$ , at the period  $t$ .

Finally, evaluating the mean of these effects  $S_{1,t}$  on  $m_{1,i}$  homologous periods (that are the same hours of each day), the seasonal coefficient  $\bar{S}_{1,i}$  is obtained:

$$\bar{S}_{1,i} = \frac{\sum_{l=0}^{m_{1,i}-1} S_{1,i+lk_1}}{m_{1,i}} \quad (4)$$

At this point, it is possible to clean up the values of the first moving average from the effect of the second seasonality with lag  $k_2$ . That is done using a second centred moving average process, with width  $k_2$  (second lag detected). As in the previous step, the effect of the second seasonality for each period ( $S_{2,t}$ ) can be calculated, and a second seasonal coefficient can be evaluated with a mean on  $m_{2,j}$  homologous periods:

$$S_{2,t} = \frac{M_{(k_1)t}}{M_{(k_2)t}} \quad (5)$$

$$\bar{S}_{2,j} = \frac{\sum_{l=0}^{m_{2,j}-1} S_{2,j+lk_2}}{m_{2,j}} \quad (6)$$

where  $M_{(k_2)t}$  is the centred moving average with width  $k_2$ , at the period  $t$ .

In our case, as it will be described in the next sections, the Double Seasonality Model (DSM) fails in following the winter/summer changes in the electricity consumption. Thus, a third coefficient is introduced by means of a corrective term, obtained dividing the average value of the measured electricity consumption in the  $h$ -th month (with  $h$  varying from 1 to 12) by the average value of the estimated trend line in the same month:

$$\bar{S}_{3,h} = \frac{\sum_{t=a_h}^{b_h} A_t}{\sum_{t=a_h}^{b_h} T_t} \quad (7)$$

where  $a_h$  and  $b_h$  are the progressive number of the first and the last hours of the  $h$ -th month in the considered dataset.

Therefore, the forecast formula of the resulting Triple Seasonality TSA model (TSM) is:

$$F_t = T_t \bar{S}_{1,i} \bar{S}_{2,j} \bar{S}_{3,h} \quad (8)$$

After the calibration phase on a given dataset, the forecast can be performed by means of a final extended formula:

$$F_t = T_t \bar{S}_{1,i} \bar{S}_{2,j} \bar{S}_{3,h} + m_e, \quad (9)$$

that includes also  $m_e$ , the mean of the error evaluated by a statistical analysis on the error, defined as observed value ( $A_t$ ) minus forecast ( $F_t$ ) in the calibration phase:

$$e_t = A_t - F_t. \quad (10)$$

### B. Detection of the presence of a lag

The presence of a periodicity in the series can be detected calculating some specific tests. In this paper the authors adopted the Ljung-Box (LB) and the Box-Pierce (BP) tests ([37], [38]). These tests verify if the data have an autocorrelation and they may exclude the presence of fully random data fluctuations. Both tests adopt the autocorrelation coefficient that may be evaluated according to the following formula:

$$r(k) = \frac{\sum_{t=1}^{n-k} (x_t - \bar{x})(x_{t+k} - \bar{x})}{\sum_{t=1}^n (x_t - \bar{x})^2}, \quad (11)$$

where  $x_t$  is the data in each period  $t$ ,  $\bar{x}$  is the mean of all the data,  $n$  is the total number of periods,  $k$  is the lag hypothesis under test. Using this coefficient, the LB test can be performed according to the following formula:

$$\chi_{LB}^2(d) = n(n+2) \sum_{k=1}^d \frac{r^2(k)}{n-k}, \quad (12)$$

where  $d$  is a chosen integer related to the number of autocorrelation coefficients under test, and it varies according to the assumed lag.

If the null hypothesis is true (absence of autocorrelation), the LB statistics is distributed according to a random variable  $\chi^2$ , with  $d$  degree of freedom.

The BP test is based on the following formula:

$$\chi_{BP}^2(d) = n \sum_{k=1}^d r^2(k), \quad (13)$$

where, again,  $n$  is the total number of periods,  $k$  is the assumed lag and  $d$  is a chosen integer, related to the number of autocorrelation coefficients under test. The two tests differ only in the different weighting systems adopted, but asymptotically converge to the same distribution.

### C. Linearity tests

A Time Series is linear if it can be expressed as a linear combination of  $Z_t$  independent random variables, with  $\psi_j$  unknown constant parameters [39]:

$$X_t = \sum_{j=-\infty}^{+\infty} \psi_j Z_{t-j}. \quad (14)$$

When this condition is not verified, the time series is nonlinear. The nonlinearity implies that the usual regressive model adopted in TSA, for instance Auto Regressive (AR) and Auto Regressive Moving Average (ARMA) models, are not adequate. It will be shown that the model presented is able to give adequate forecasts of the energy consumption, even if the time series is not linear.

In order to check the linearity presence, some proper tests can be performed. In this paper, the authors adopt the Lee-White-Granger (LWG) test [40] and the Terasvirta-Lin-Granger (TLG) test [41].

### D. Stationarity tests

A Time Series is (weakly) stationary if the mean does not depend on time and if the autocovariance function is independent of  $t$  for each lag [39].

In order to check the stationarity of the time series, some tests can be performed (based on the detection of the presence of unit roots). In this paper, the Augmented Dickey-Fuller (ADF) [42] and Phillips-Perron (PP) [43] tests are proposed and applied to the energy consumption time series.

The results of these tests will show that the series under study is stationary.

### E. Error metrics

Two possible error metrics that can evaluate the model performances, already adopted in [16, 17, 31], are the *Mean Percentage Error* (MPE) and the *Coefficient of Variation of the Error* (CVE).

The MPE gives a measurement of the error distortion, i.e. is able to describe if the model overestimates or underestimates the observed data.

The CVE, instead, considers the variation from the observed data in absolute value. In other words, it provides the error dispersion. Those metrics are evaluated according to the following formulas:

$$MPE = \frac{\sum_{t=1}^n \left( \frac{A_t - F_t}{A_t} \right) 100}{n} \quad (15)$$

and

$$CVE = \frac{\sqrt{\frac{\sum_{t=1}^n (e_t)^2}{n-1}}}{\bar{A}}, \quad (16)$$

where  $\bar{A}$  is the mean value of the actual data in the considered time range,  $n$  is the number of data.

## III. CASE STUDY

Electricity consumption of the local transportation in Sofia (Bulgaria) is considered as a case study.

In the hauler *Transenergo*, the Power Engineer has to declare necessary electricity consumption for every hour of the following week. The incorrect request affects the price of the electricity. Electricity consumption is a random process which depends on many factors. The Power Engineer has information for the following data: kilometers run, temperature, the kind of day and from this information has to declare the necessary electricity consumption [4].

The data of consumption, in MWh, are provided by an electronic energy meter that measures the hourly electricity consumption during night and daytime. The dataset is related to 2011, 2012 and 2013 years; in particular, the period that goes from the 1<sup>st</sup> of January 2011 to the 31<sup>st</sup> of December 2012 has been used in the model calibration phase, and data

collected in January 2013 have been adopted for the validation of the final model.

The electrical transport in Sofia started in 1901. Currently in Sofia electrical trams and trolleybuses are a relevant part of the public transportation, carrying each year, millions of passengers. In 2008, for instance, over 198 million of passengers have been transported [44].

Power is delivered by 24 rectifier stations with a total installed capacity of over 125950 kW. The network consists of over 263 km tram tracks and 257 km trolley tracks, and the cable network is more than 740 kilometers [44].

Since summer and winter exploit a strong variation in average temperatures, with a consequent different usage of electrical heating system, and since in summer transportation schedule a smaller number of vehicles is used, a seasonal variation in electricity consumption is expected. The same occurs for week (working) days and weekend days (and public holidays), such as for day and night variations. This suggests weekly and daily periodicities.

In general, in the last decades, electricity consumption in Bulgaria has been growing but, thanks to the operating nuclear plants, the country satisfied the internal request and was able to export part of the produced electrical power. However, since 2006, the export of electricity has been reduced because of the closure of two older nuclear units. This energy production changes requires a more effective management of local consumptions.

#### IV. DATA ANALYSIS AND RESULTS

The first step, in order to build the model, is to analyse the dataset to be used in the calibration phase. The first choice was to consider the hourly electricity consumption, measured during all the year 2011. Once this test has been performed, a long term analysis can be pursued, adopting 2011 and 2012 data as calibration dataset and validating the model on a given validation dataset in 2013.

##### A. Calibration on 2011 dataset

The first calibration dataset is made of 8760 hourly electricity consumptions, measured in MWh, and the summary statistics are resumed in Table 1.

As it can be noticed from skewness and kurtosis values, the distribution is normal. In addition, the high value of standard deviation with respect to the mean, together with the maximum and minimum values, exploits a very spread distribution.

The load duration curve, i.e. the plot of energy consumption (sorted in descending order) versus the number of hours in which that value of consumption is obtained and surpassed, is reported in Fig. 1.

**Table 1:** Summary of statistics of the 2011 calibration data set, 8760 data, in Megawatt hour.

Mean [MWh]	Std.dev [MWh]	Median [MWh]	Min [MWh]	Max [MWh]	skew	kurt
5.14	3.12	5.28	0.22	12.62	0.17	-0.75

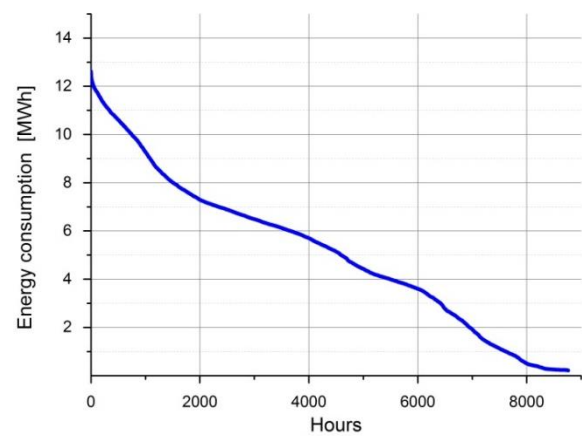


**Fig. 1:** Electricity consumption in 2011 sorted by descending order of magnitude. The x axis reports the number of hours in which the corresponding electrical consumption is exceeded.

**Table 2:** Ljung-Box and Box-Pierce tests performed on the 8760 measurements of the 2011 calibration dataset.

Test	$\chi^2$	$d$	$p$ -value
Ljung-Box	53542.33	30	< 2.2e-16
Box-Pierce	78500.02	50	< 2.2e-16

**Table 3:** Lee-White-Granger (LWG) and Terasvirta-Lin-Granger (TLG) tests for linearity performed on the 8760 measurements of the 2011 calibration dataset.

Test	Statistic of the test	$df$	$p$ -value
LWG	37.4105	2	7.524e-09
TLG	35.4774	2	1.978e-08

In the previous section, it has been discussed the probable presence of three periodicities, a daily one, a weekly one and a seasonal one (implemented on a monthly base). In order to check if the data are autocorrelated or not, the Ljung-Box (LB) and Box-Pierce (BP) tests have been performed (see Subsection II.B). Results are reported in Table 2, in which the small  $p$ -values in both tests, i.e. the very small probability to observe the sample if the null hypothesis is true, indicates that the hypothesis of absence of autocorrelation in the data can be rejected.

The linearity tests proposed in the Section II.C, are performed on the time series under study, in the  $R$  software framework. The resulting very low probability values, reported in Table 3, suggest to reject the null hypothesis, i.e. the linearity of the time series. The tests result and the good performances of the model presented in this section highlight its capability of reproducing the nonlinear feature of the time series.

The autocorrelation of the data has been evaluated by means of an autocorrelation plot (correlogram), reported in Fig. 2. It is evident the presence of several periodicities. In particular the maximum values of the autocorrelation are obtained in correspondence of a lag (period) of 24 hours (daily periodicity) and 168 hours (weekly periodicity). The latter periodicity is confirmed by the highest autocorrelation value in the correlogram of the first moving average data, calculated with 24 hours span (Fig. 3).

Figures 4, 5 and 6 report the auto dispersion plots of three different datasets: in all cases that data are clustered around the bisector, confirming the presence of the presumed lag. Figure 4 reports the observed dataset and it is plotted as a function of the same data shifted by 24 hours. Two patterns are evident out from the bisector line, showing that more periodicities are present. Figure 5 reports the auto dispersion of the observed dataset as a function of the same data shifted by 168 hours, i.e. one week. Again, the data follow the bisector, but still some of them seem to be not randomly distributed. Figure 6, instead, reports the centred moving average data (span 24), plotted versus the same data shifted by 168 hours (one week). The plot shows a general gathering along the bisector line, with some variations that are mostly symmetric with respect to the bisector. This result confirms the presence of a further periodicity, with low frequency.

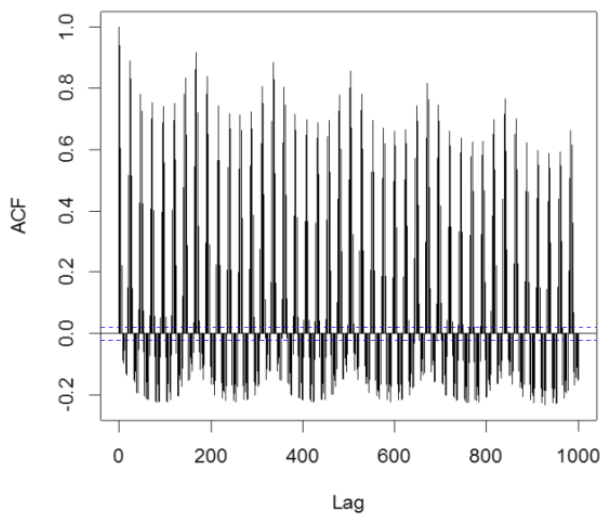


**Fig. 2:** Autocorrelation plot (correlogram) of the 2011 data as a function of the lag (periodicity).

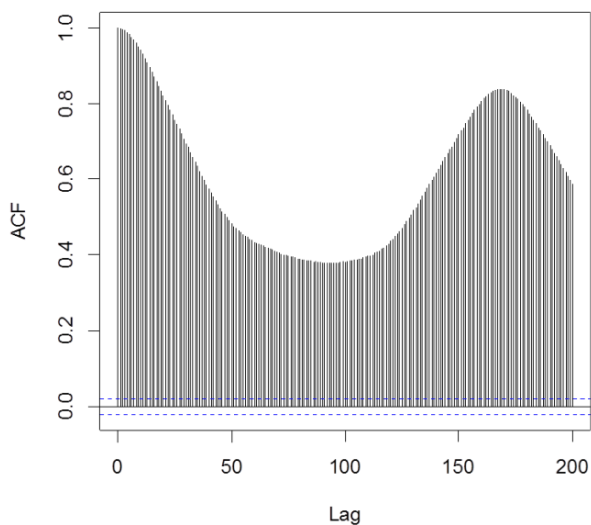


**Fig. 3:** Correlogram for the first centred moving average data, performed on the 2011 dataset. The value of autocorrelation coefficient is plotted as a function of the lag.

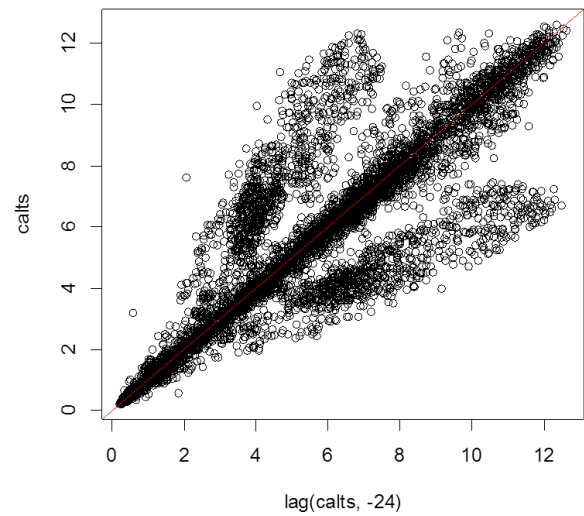


**Fig. 4:** Auto dispersion plot of the 2011 electricity consumption dataset plotted as a function of the same data shifted by 24 hours.

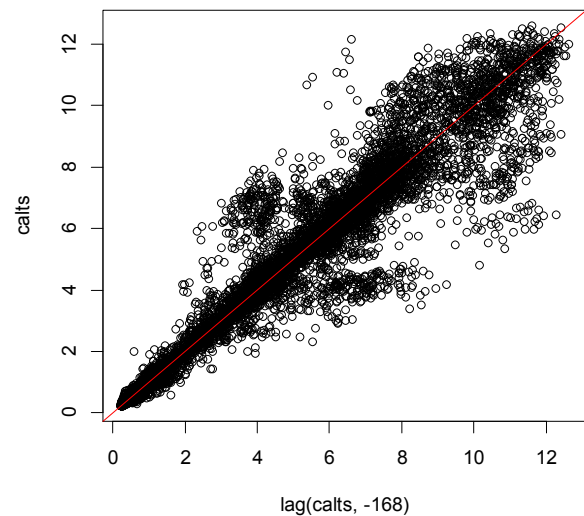


**Fig. 5:** Auto dispersion plot of the 2011 electricity consumption dataset plotted as a function of the same data shifted by 168 hours.

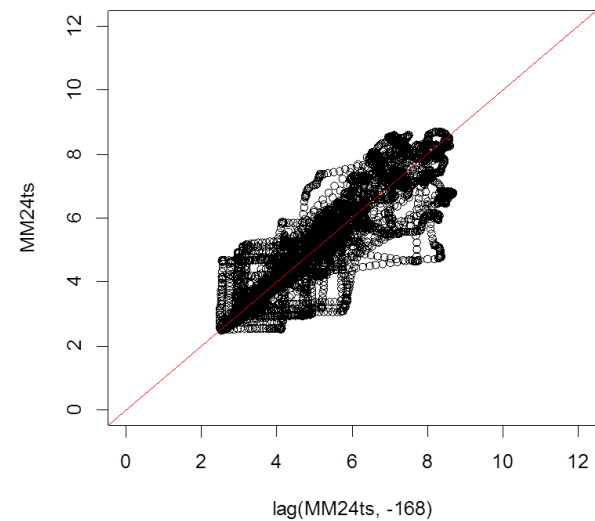


**Fig. 6:** Auto dispersion plot of the moving average with span 24 plotted as a function of the same moving average data shifted by 168 hours, in the 2011 calibration dataset.

Once the periodicities have been detected, the model has been built as described in Section II. The moving averages are plotted in Figure 7, together with the trend line.

The set of TSA model parameters, that are trend line parameters and 24 first seasonality (daily) coefficients, is reported in Table 4 and Figure 8, while the 168 second seasonality (weekly) coefficients are plotted in Figure 9.

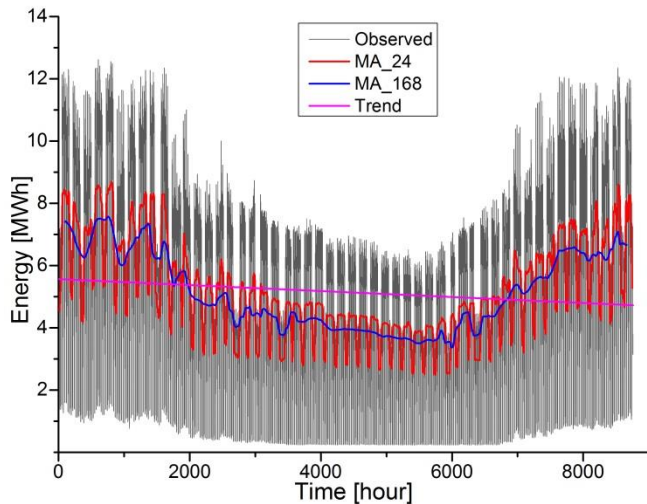


**Fig. 7:** Plot of the two centred moving averages and of the trend line. In black the actual 2011 data, in violet the trend line, in red the first moving average (span 24), in blue the second moving average (span 168).

**Table 4:** Model parameters estimated on the 2011 electricity consumption data.  $b_0$  and  $b_1$  are respectively the intercept and the slope of the trend line, while  $\bar{S}_i$  is the hourly coefficient, to reconstruct the daily periodicity, in the time range from  $i-1$  to  $i$  hour.

Time Series Model parameters			
$b_0$	5.55998	$b_1$	-0.0000957
$\bar{S}_1$	0.14318	$\bar{S}_{13}$	1.38711
$\bar{S}_2$	0.10604	$\bar{S}_{14}$	1.28621
$\bar{S}_3$	0.10540	$\bar{S}_{15}$	1.22370
$\bar{S}_4$	0.11779	$\bar{S}_{16}$	1.26628
$\bar{S}_5$	0.42944	$\bar{S}_{17}$	1.28007
$\bar{S}_6$	0.97802	$\bar{S}_{18}$	1.35565
$\bar{S}_7$	1.26947	$\bar{S}_{19}$	1.41998
$\bar{S}_8$	1.47812	$\bar{S}_{20}$	1.39447
$\bar{S}_9$	1.43660	$\bar{S}_{21}$	1.22622
$\bar{S}_{10}$	1.36739	$\bar{S}_{22}$	0.80087
$\bar{S}_{11}$	1.38302	$\bar{S}_{23}$	0.60751
$\bar{S}_{12}$	1.41843	$\bar{S}_{24}$	0.46727

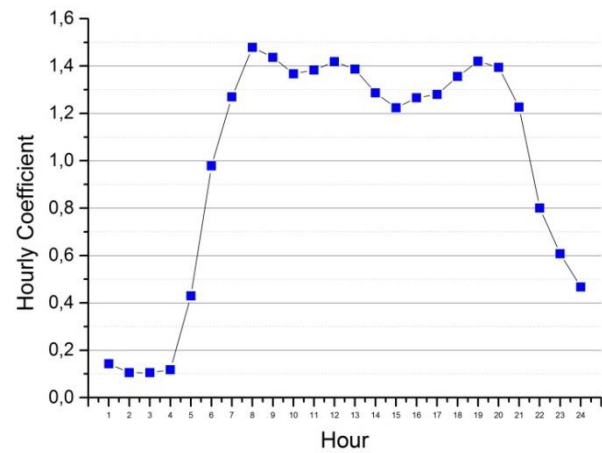


**Fig. 8:** Hourly coefficient used to reconstruct the daily periodicity in the 2011 dataset.

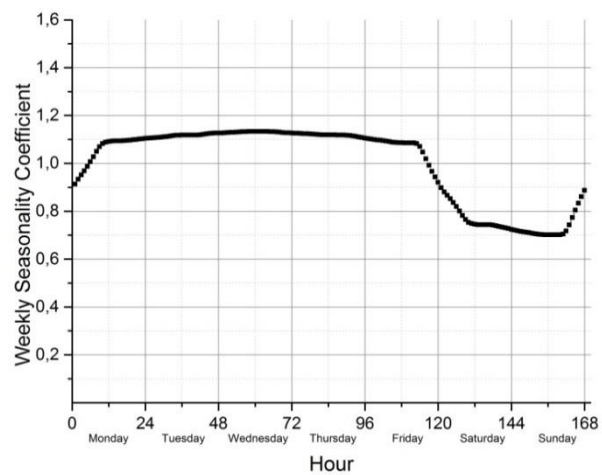


**Fig. 9:** Hourly coefficient used by the model to reconstruct the weekly periodicity in the 2011 dataset.

With this procedure, a Double Seasonality TSA Model (DSM) has been built. The result of the forecast of the DSM are shown in Figure 10, together with the observed values dataset. It is easy to notice that even if the model forecasts follow the local (daily and weekly) oscillation, there is a long term (low frequency) periodicity to be still included. As reported in section II, a third coefficient, in charge of describing the monthly seasonal behavior of the data, is introduced. This corrective coefficient is calculated according to formula (7), i.e. dividing the average value of the measured electricity consumption in each month by the average value of the estimated trend line in the same month.

These 12 ratios are able to describe the long term variations of the time series. The resulting monthly coefficients are plotted in Figure 11 and exploit the higher electricity consumption observed during cold months, probably due to higher number of vehicles running and to heating systems.

The application of the third seasonal coefficient to the DSM, produce a Triple Seasonality TSA Model (TSM) whose forecasts are plotted in Fig. 12 together with the observed data.

In order to better depict the improvement produced by the third seasonal coefficient, a plot of the DSM and TSM

forecasts and of the observed data, in the summer time range (from 4000 to 4500 hours), is reported in Figure 13.

The TSM better agrees with the observed data in quite all the range, while the DSM model underestimates during winter time and overestimate in summer months. Few local oscillations are lost.

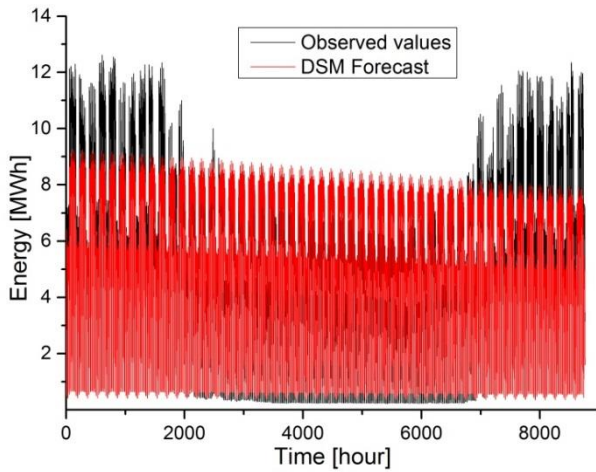


**Fig. 10:** Observed electricity consumption and Double Seasonality TSA model results, plotted in 2011 time range.

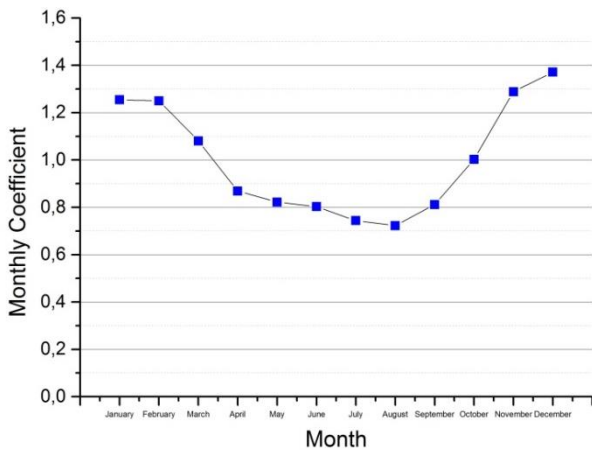


**Fig. 11:** Monthly coefficient used by the model to reconstruct the third seasonal behaviour of the electricity consumption in 2011.

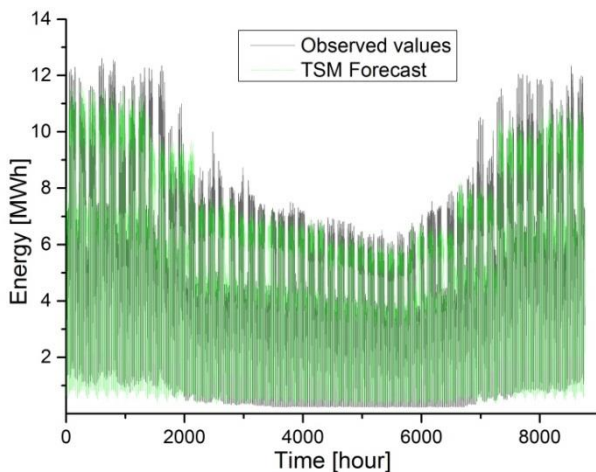


**Fig. 12:** Observed electricity consumption and Triple Seasonality TSA model, plotted in 2011 time range.

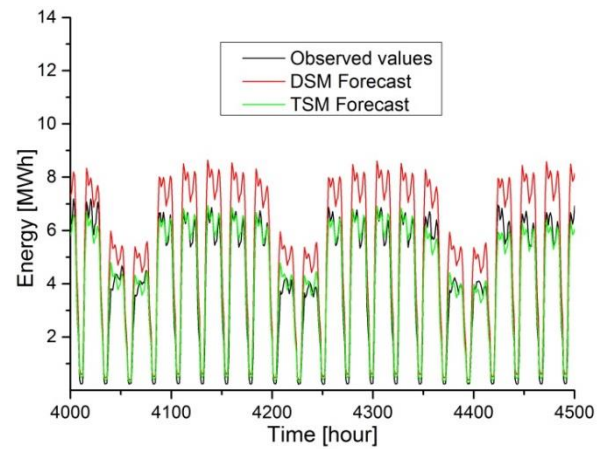


**Fig. 13:** Observed (black line) and predicted electricity consumption according to DSM (red line) and TSM (green line), during 2011: zoom on the time range from 4000 to 4500 hours.

**B. Calibration on 2011 and 2012 dataset**

The second calibration dataset is made of 17544 hourly electricity consumption data, measured in MWh, and the summary statistics are resumed in Table 5. Again, such as in Section IV.A, skewness and kurtosis values suggest that the distribution is normal. An important consideration is that, even if the dataset size is doubled adding 2012 data, the statistics of the dataset are practically the same. This is an evidence of the stationary behaviour of the time series, as it will be confirmed by the stationarity tests.

**Table 5:** Summary of statistics of the 2011 and 2012 calibration data set, 17544 data, in Megawatt hour.

Mean [MWh]	Std.dev [MWh]	Median [MWh]	Min [MWh]	Max [MWh]	skew	kurt
5.16	3.18	5.25	0	13.81	0.24	-0.64

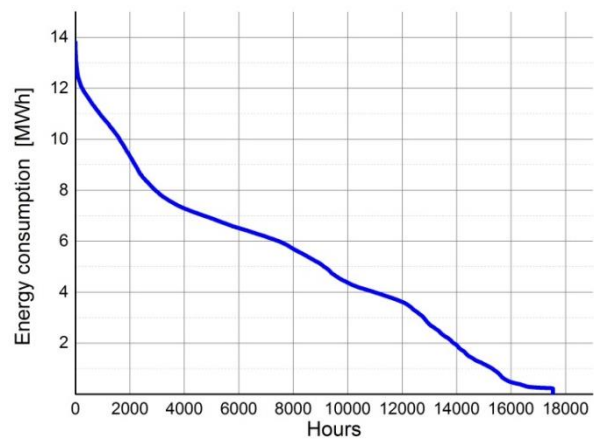


**Fig. 14:** Electricity consumption in 2011 and 2012 sorted by descending order of magnitude. The x axis reports the number of hours in which the corresponding electrical consumption is exceeded.

The load duration curve of the 2011 and 2012 dataset is reported in Fig. 14. Let us remind that the x axis values represent the number of hours in which that value of consumption is obtained and surpassed.

The results of the tests summarized in Section II, are reported in Tables 6, 7 and 8. The presence of autocorrelation and the nonlinearity in the series is confirmed by LB and BP, and by WLG and TLG tests.

The low p-value of the ADF and PP tests (Table 8) highlights the absence of unit roots in the process, this evidence confirms the hypothesis that the process is stationary: it does not have significant changes in the mean and variance depending on the considered period.

**Table 6:** Ljung-Box and Box-Pierce tests performed on the 17544 measurements of the calibration dataset.

Test	$\chi^2$	$d$	$p$ -value
Ljung-Box	109874.6	30	2.2e-16
Box-Pierce	160968.7	50	2.2e-16

**Table 7:** Lee-White-Granger (LWG) and Terasvirta-Lin-Granger (TLG) test for linearity performed on the 17544 measurements of the calibration dataset.

Test	Statistic of the test	df	$p$ -value
LWG	78.086	2	2.2e-16
TLG	76.624	2	2.2e-16

**Table 8:** Augmented Dickey-Fuller and Phillips-Perron Unit Root tests for stationarity of the time series performed on the 17544 measurements of the calibration dataset.

Test	Statistic of the test	Lag	$p$ -value
Augmented Dickey-Fuller	-10.2615	25	0.01
Phillips-Perron	-27.1904	14	0.01

Figures from 15 to 19 show that the 2011 and 2012 data time series has the same features of the single year calibration dataset, suggesting that the model built on the new dataset will be similar to the previous one (Section IV.A).

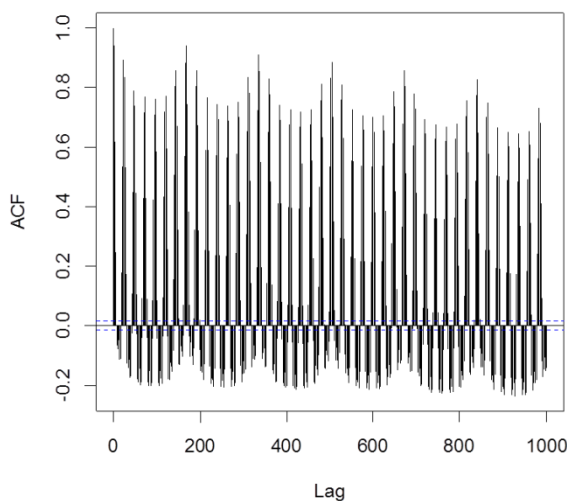


**Fig. 15:** Autocorrelation plot (correlogram) as a function of the lag (periodicity) in 2011 and 2012 dataset.

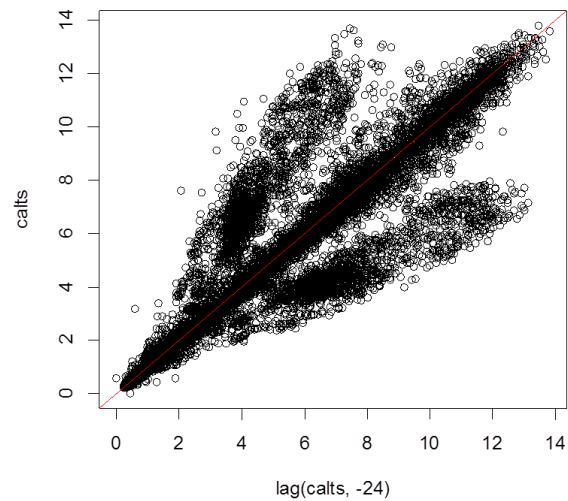


**Fig. 16:** Auto dispersion plot. The power absorption dataset is plotted as a function of the same data shifted by 24 hours.

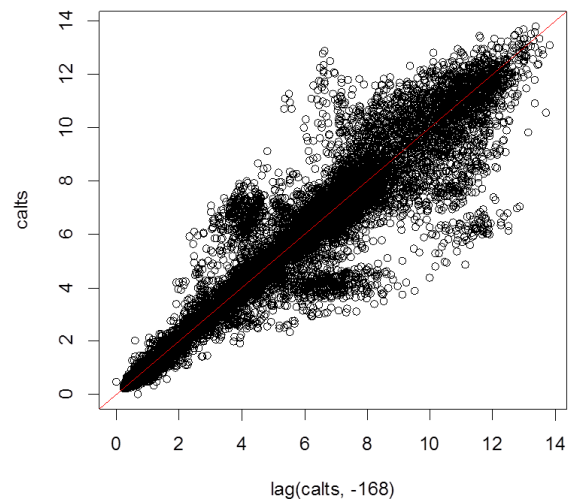


**Fig. 17:** The power absorption dataset is plotted as a function of the same data shifted by 168 hours.

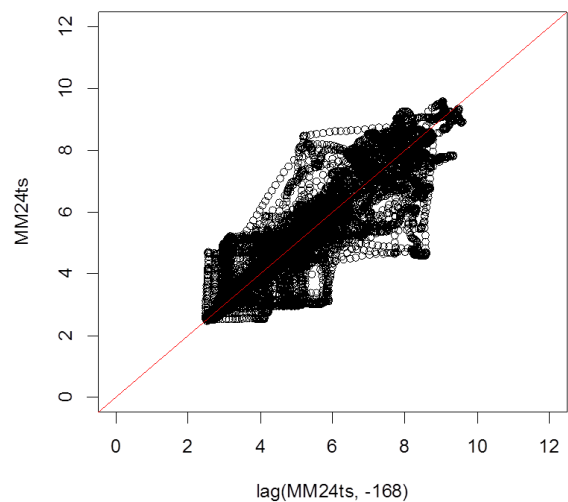


**Fig. 18:** Auto dispersion plot. The moving average with span 24 is plotted as a function of the same moving average considering each data shifted by 168 days.

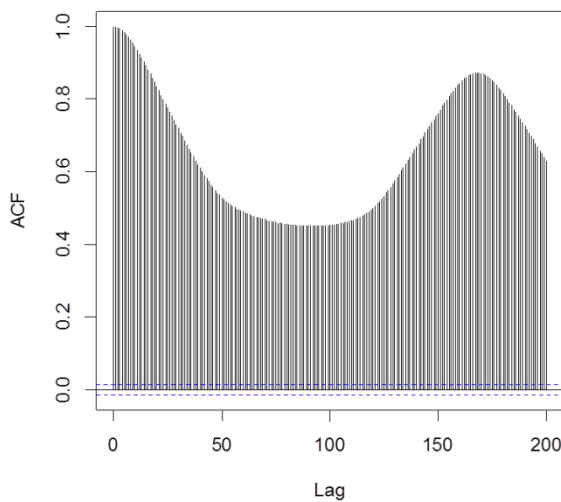


**Fig. 19:** Correlogram plot for the first centred moving average data (with span 24). The value of autocorrelation coefficient is plotted as a function of the lag.

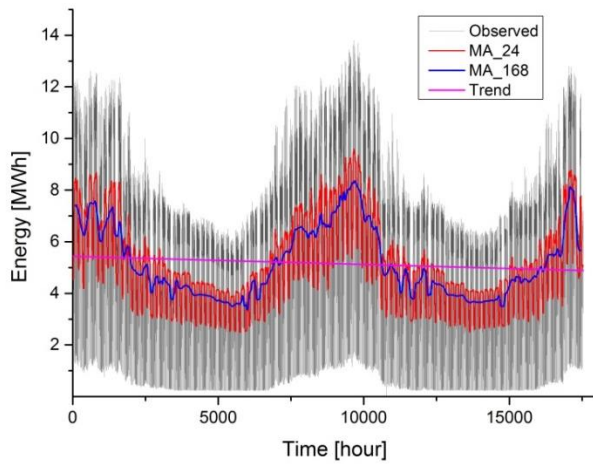


**Fig. 20:** Centred moving averages and trend line plot. In black the actual data of 2011 and 2012, in violet the trend line, in red the first moving average (span 24), in blue the second moving average (span 168).

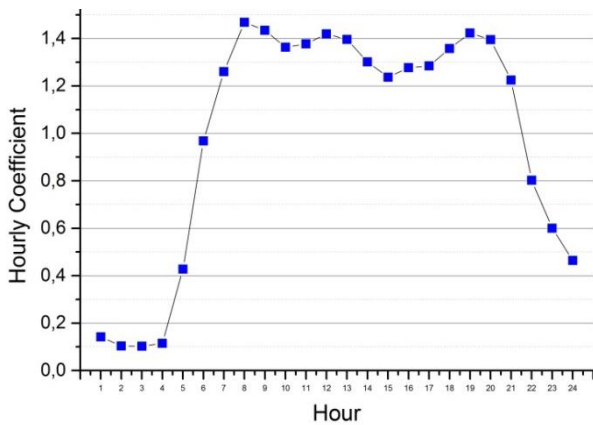


**Fig. 21:** Hourly coefficient used to reconstruct the daily periodicity in the 2011 and 2012 dataset.

Once the multiple seasonality has been detected, the moving averages and trend (Figure 20) have been computed, and the parameters have been evaluated (see Table 9 and Figures 21, 22 and 23), the model can be drawn and superimposed on the actual data (Figure 24).

**Table 9:** Model parameters estimated on the 2011 and 2012 power absorption data.  $b_0$  and  $b_1$  are respectively the intercept and the slope of the trend line, while  $\bar{S}_i$  is the seasonal coefficient in the time range from  $i-1$  to  $i$  hour.

Time Series Model parameters			
$b_0$	5.4329841	$b_1$	-3.129E-05
$\bar{S}_1$	0.14232	$\bar{S}_{13}$	1.39581
$\bar{S}_2$	0.10372	$\bar{S}_{14}$	1.30130
$\bar{S}_3$	0.10293	$\bar{S}_{15}$	1.23696
$\bar{S}_4$	0.11504	$\bar{S}_{16}$	1.27697
$\bar{S}_5$	0.42737	$\bar{S}_{17}$	1.28428
$\bar{S}_6$	0.96794	$\bar{S}_{18}$	1.35810
$\bar{S}_7$	1.26038	$\bar{S}_{19}$	1.42362
$\bar{S}_8$	1.46817	$\bar{S}_{20}$	1.39512
$\bar{S}_9$	1.43488	$\bar{S}_{21}$	1.22463
$\bar{S}_{10}$	1.36337	$\bar{S}_{22}$	0.80240
$\bar{S}_{11}$	1.37740	$\bar{S}_{23}$	0.60029
$\bar{S}_{12}$	1.41945	$\bar{S}_{24}$	0.46441

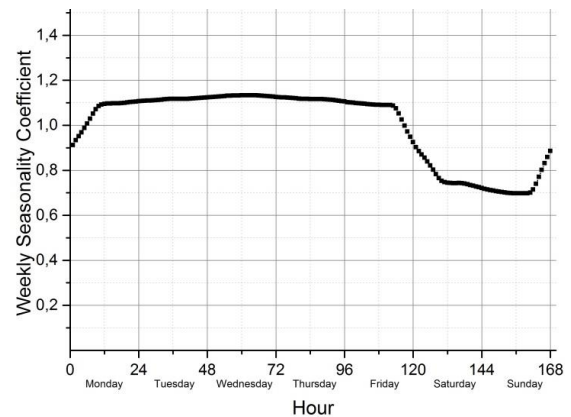


**Fig. 22:** Hourly coefficient used by the model to reconstruct the weekly periodicity in the 2011 and 2012 dataset.

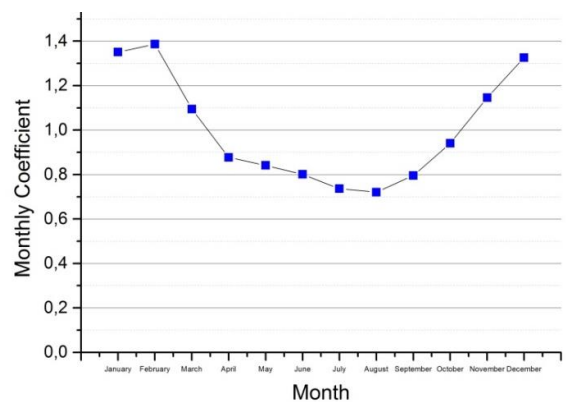


**Fig. 23:** Monthly coefficient used by the model to reconstruct the third seasonal behaviour of the electricity consumption in 2011 and 2012.

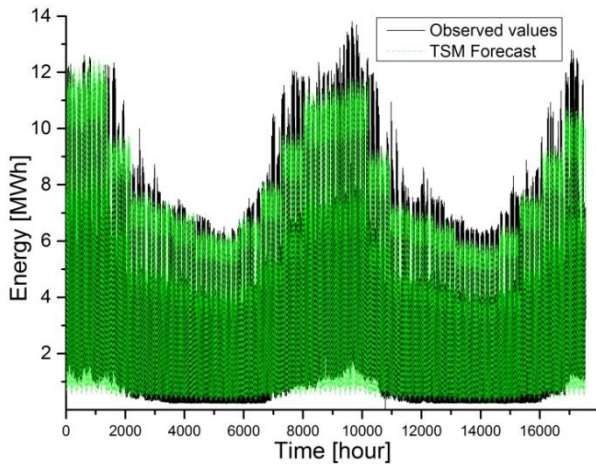


**Fig. 24:** Observed and predicted power absorption, during the years 2011 and 2012 (i.e. calibration dataset). The black line are the observed values in 2011 and 2012, the green line is obtained by triple seasonality model.

The two years calibration gave results very similar to 2011 calibration, confirming the stationarity of the series and the strong periodic pattern. The most important improvement is related to the third coefficient (the one in charge of reproducing the monthly differences), that has been computed on a greater dataset.

V. ERROR ANALYSIS AND VALIDATION

In order to quantify the performances of the model calibrated on different dataset, an error analysis has been done both on DSM and TSM, in 2011 dataset, and on TSM in 2011 and 2012 dataset. In addition, a validation of the latter model, i.e. TSM calibrated on 2011 and 2012 data, has been performed on 744 data of January 2013, so that the forecasting capabilities of the model in a time range not included in the calibration can be evaluated.

Let us remind that the error is calculated according to Formula 10 (Subsection II.A).

A. Error analysis on 2011 calibration dataset

Comparing the error statistics of Double (DSM) and Triple (TSM) Seasonality Models (Table 10), it can be noticed that the standard deviation strongly decreases when moving from DSM to TSM. Also the median and the spread between minimum and maximum error improve when introducing the third periodicity.

**Table 10:** Summary of statistics of the error distribution in the Double Seasonality Model (DSM) and Triple Seasonality Model (TSM), evaluated on the 2011 calibration dataset; results are given in MWh.

Model	Mean [MWh]	Std.dev [MWh]	Median [MWh]	Min [MWh]	Max [MWh]
DSM	0.02	1.49	-0.25	-4.86	4.92
TSM	0.02	0.81	0.03	-3.99	3.6

In DSM case, the histogram of errors (Figure 25) is right skewed, while in TSM case the distribution (Figure 26) is more Gaussian-like, suggesting that after introducing the third coefficient the errors are randomly distributed.

Then, in Figures 27 and 28 respectively the correlogram of the DSM and the TSM errors are reported. It is evident that in the DSM case the errors are still strongly autocorrelated, while in TSM, thanks to the adoption of the third seasonal coefficient, this effect is clearly reduced.

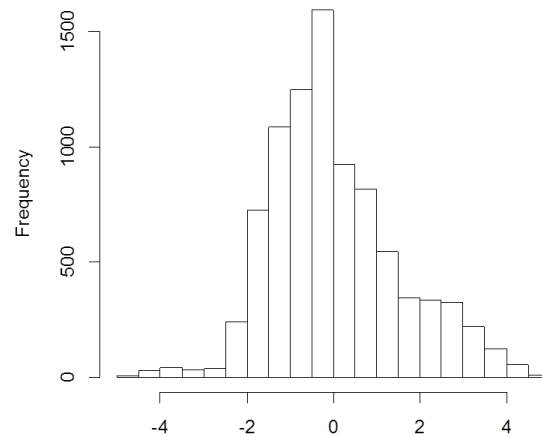


**Fig. 25:** Frequency histogram of the errors calculated on the Double Seasonality Model, performed on the 8760 calibration data (2011).

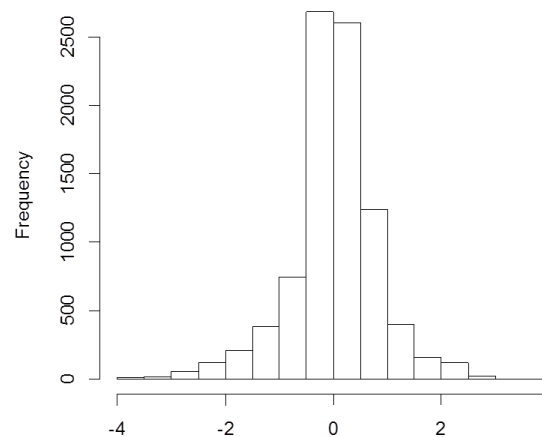


**Fig. 26:** Frequency histogram of the errors calculated on the triple seasonality model, performed on the 8760 calibration data (2011).

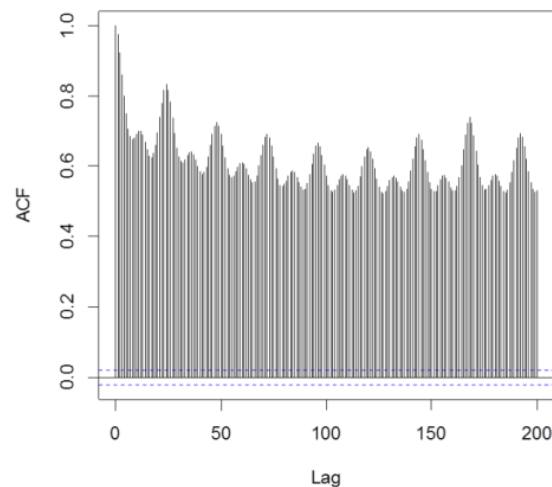


**Fig. 27:** Correlogram for the errors, Double Seasonality Model calibrated on 2011 dataset. The value of autocorrelation coefficient is plotted as a function of the lag.

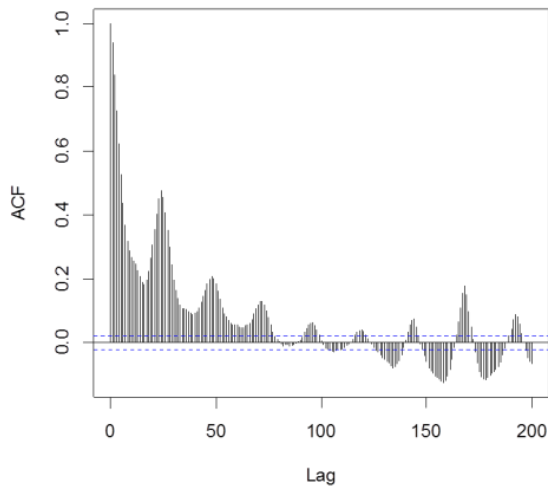


**Fig. 28:** Correlogram for the errors, Triple Seasonality Model calibrated on 2011 dataset. The value of autocorrelation coefficient is plotted as a function of the lag.

*B. Error analysis on 2011 and 2012 calibration dataset*

The second error analysis has been pursued following the same procedure as in subsection 5.1. The error statistics are reported in Table 11. Since the DSM again is worse than TSM, and since it has been largely demonstrated that it is not effective in this energy consumption time series, the authors will consider only the TSM for following analysis and validation.

The frequency histogram, the Q-Q plot and the autocorrelation plot related to TSM are reported respectively in Figures 29, 30 and 31. Both the histogram and the symmetry in the Q-Q plot show that the error is quite normal distributed. The error correlogram, Fig. 31, still presents a residual autocorrelation, greater than the one observed on 2011 dataset.

**Table 11:** Summary of statistics of the error distribution in the Double Seasonality Model (DSM) and Triple Seasonality Model (TSM), evaluated on the 2011 and 2012 calibration dataset, in MWh.

Model	Mean [MWh]	Std.dev [MWh]	Median [MWh]	Min [MWh]	Max [MWh]
DSM	0.02	1.6	-0.3	-5.23	7.11
TSM	0.02	0.9	0	-4.54	5.22

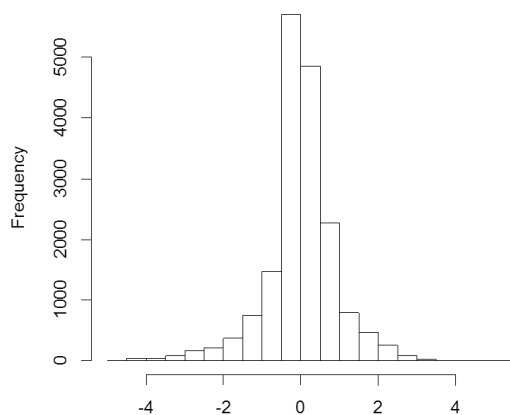


**Fig. 29:** Frequency histogram of the errors calculated on the Triple Seasonality Model calibration dataset, performed on the 17544 dataset (2011 and 2012 years).

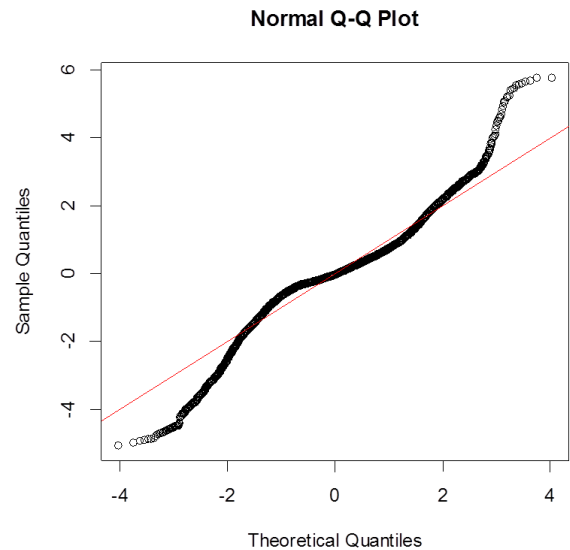


**Fig. 30:** Normal probability plot that describe error behavior of the Triple Seasonality Model applied to the 17544 calibration data (2011 and 2012 years).

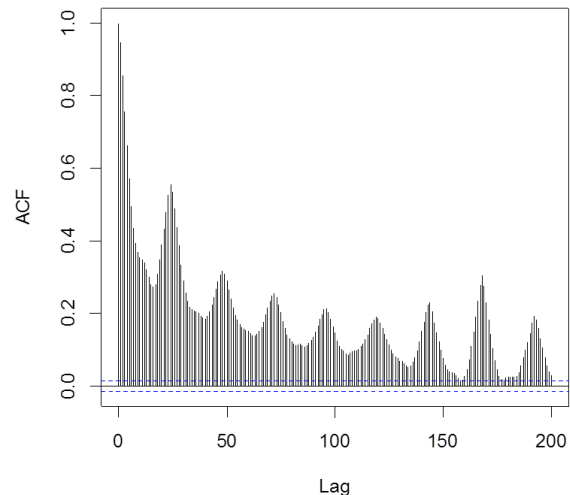


**Fig. 31:** Correlogram plot for the errors for the Triple Seasonality Model calibrated on 2011 and 2012 dataset. The value of autocorrelation coefficient is plotted as a function of the lag.

*C. Validation on January 2013 dataset*

In order to understand if the Triple Seasonality Model is suitable to forecast future values of energy consumption, a comparison between model forecasts and actual values (not included in the calibration phase) has been performed. The choice was to adopt 744 energy consumption data related to January 2013 (i.e. the period closest to the calibration range).

A plot of the results of the validation is reported in Figure 32, where the actual data (black line) and the forecasts (green line) are plotted versus time. The model forecast line has a good agreement with the observed one, except for the first part of the interval (i.e. the first day of the year), in which, probably due to holiday bus schedule, a different slope is observed, more similar to weekend slope. Of course, the TSM cannot predict local changes in the periodic pattern, since it is tuned on the entire dataset (in this case, on 2011 and 2012 dataset). This disagreement is evidenced in the error statistics

(Table 12), in particular looking at the spread between minimum and maximum, and in the error histogram (Figure 33), in which there is a quite long left tail. This tail can be seen also in the Q-Q plot (Figure 34), in the underestimation of the first quantiles.

Beside this particular problem, the error is distributed according to a normal distribution and it is very low autocorrelated (Fig. 35), showing that it is almost randomly distributed. Thus, the model does not have any recursive effect and has a good predictive performance.

The error metrics, defined in Subsection II.E, evaluated on the validation dataset, both for DSM and TSM, confirm the improvement in the prediction when introducing the third coefficient in the model.

**Table 12:** Summary of statistics of the error distribution, Triple Seasonality Model, evaluated on the validation dataset (January 2013), in MW.

Mean [MW]	Std.dev [MW]	Median [MW]	Min [MW]	Max [MW]
-0.04	1.16	0.2	-6.5	2.58

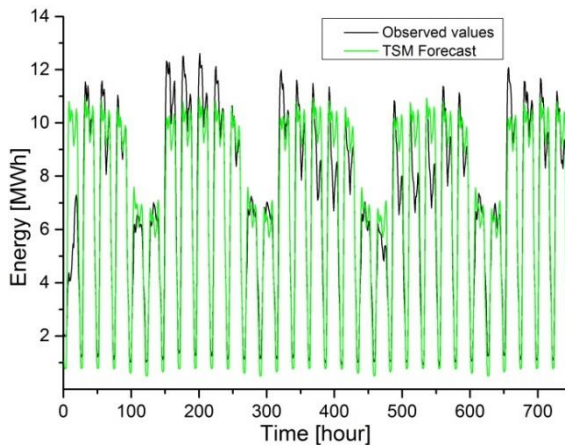


**Fig. 32:** Observed and predicted power absorption during the validation period, the 744 hours of January 2013. The black line are the observed values, the green line is obtained by Triple Seasonality Model.

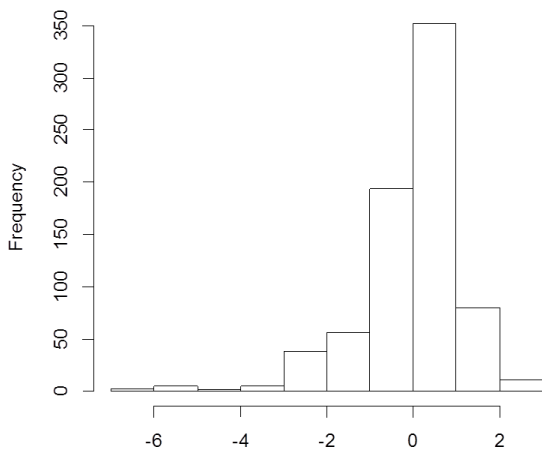


**Fig. 33:** Frequency histogram of the errors calculated on the Triple Seasonality Model validation dataset, performed on the 744 data.

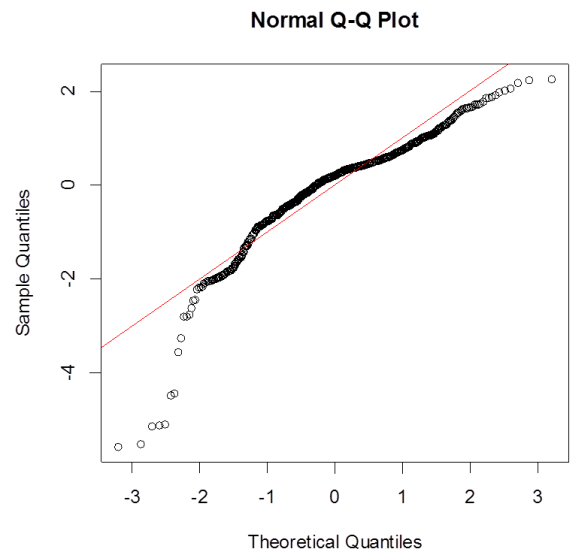


**Fig. 34:** Normal probability plot that describe error behaviour of the Triple Seasonality Model applied to the 744 validation data.

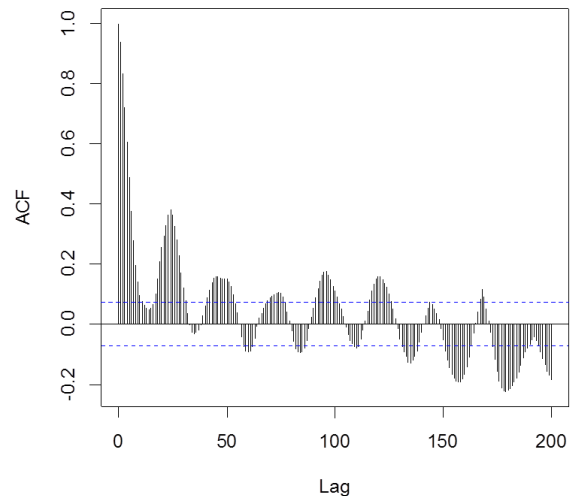


**Fig. 35:** Correlogram plot for the errors, evaluated in the validation phase (January 2013), of the Triple Seasonality Model. The value of autocorrelation coefficient is plotted as a function of the lag.

**Table 13:** MPE and CVE (error metrics) values, calculated in the validation phases, for the two different models.

Type of model	Dataset	MPE	CVE
Double seasonality	744 validation data	27.9	0.322
Triple seasonality	744 validation data	2.9	0.175

## VI. CONCLUSIONS

In this paper the authors presented an innovative model based on Time Series Analysis and its application to the electricity consumption of public transportation in Sofia (Bulgaria).

The importance of prediction of energy consumption is mainly related to the advantages in the business of main users. The dataset adopted in this paper consisted in the energy consumption of trolleybuses and trams in Sofia, measured in 2011, 2012 and 2013. The performance of Ljung-Box and Box-Pierce statistical tests allowed to detect a periodicity in

the series and to exclude a pure random behavior of the data. The study of correlograms highlighted the maximums of the autocorrelation function, thus being able to observe the correct frequency to be reproduced. Augmented Dickey-Fuller and Phillips-Perron statistical tests made it possible to rule out the presence of unit roots and to lean towards the stationarity of the series.

The model proposed in this paper to reproduce the slope of the series is made of a trend component, estimated by a parametric function, and of a seasonal component, obtained by multiplicative coefficients calculated with non-parametric methods. These seasonal coefficients are able to reproduce the different observed frequencies in the series. In particular, two models have been presented: a first one with two seasonal coefficients (Double Seasonality Model, DSM) and a second one that adds a third monthly coefficient (Triple Seasonality Model, TSM).

A preliminary analysis was performed on power consumption data measured in 2011: in this calibration phase, the results of DSM and TSM predictions were compared both in terms of graphical agreement with observed data and of error distribution analysis, i.e. the analysis of the difference between observed values and forecasts. The improvement obtained with the implementation of TSM and the strong reduction of autocorrelation in the error dataset, with respect to DSM case, have been clearly evidenced.

Even if the application of Lee-White-Granger and Teräsvirta-Lin-Granger statistical tests on the dataset allowed to reject the null hypothesis of linearity of the series, the TSM fully achieved the aim of reproducing the behavior of the data used in the calibration, in terms of general trend and periodicities.

Thus, the TSM has been tested on a broader series by performing a calibration on data from the years 2011 and 2012. As it could be expected, due to the stationarity of the series and to the high value of the autocorrelation function maximum, adding the 2012 data to the analysis, little changes have been observed in the seasonal coefficients used to reproduce daily and weekly periodicities (high and medium frequencies).

On the contrary, the third coefficient (low frequency), that decisively move away from the neutral value of the unit in the various months, benefited of a larger calibration dataset, with a better evaluation.

Finally, the forecasting TSM has been validated on a period of power consumption not used in the previous phase of model calibration (January 2013, i.e. 744 hours). The good performances have been highlighted by means of graphical comparison, very low error mean and standard deviation, quite normal error distribution, low values of Mean Percentage Error (MPE) and Coefficient of Variation of the Error (CVE).

Besides the good results of the model, also in the validation phase, its coefficients can be used to better understand the consumptions behavior in different seasons and conditions. For instance, regarding the raise of consumption during winter time, the percentage of absorption due to heating system can be studied according to the monthly coefficients, in order to understand if a load curtailment process can be performed.

Further investigation can be the comparison of the presented model with other approaches, such as, for instance, neural network, genetic algorithm, multivariate regression, etc..

## REFERENCES

- [1] Deng S. J., Oren S. and Gross G., "Design and Valuation of Demand Response Mechanisms and Instruments for Integrating Renewable Generation Resources in a Smart Grid Environment", in *PSERC Report* 12-24, September 2012.
- [2] Mancarella P., Chicco G., "Real-time demand response from energy shifting in Distributed Multi-Generation", *IEEE Transactions on Smart Grid*, 4 (2013) 1928-1938.
- [3] <http://energy.gov/oe/technology-development/smart-grid/demand-response> (November 2014)
- [4] Iliev S., Popova S., "Electricity Consumption Prediction System for the Public Transportation", *WSEAS Transactions on Systems*, 13 (2014) 638-643.
- [5] Popova S., Iliev S., Trifonov M., "Neural Network Prediction of the Electricity Consumption of Trolleybus and Tram Transport in Sofia City", in *Latest Trends in Energy, Environment and Development, Proc. of the Int. Conf. on Urban Planning and Transportation (UPT'14)*, Salerno (Italy), June 2014, pp. 116-120.
- [6] Morano, P., Tajani, F., "Bare ownership evaluation. Hedonic price model vs. artificial neural network", *International Journal of Business Intelligence and Data Mining*, Vol. 8, No. 4, (2013), pp. 340-362.
- [7] Chen B.J., Chang M.W., Lin C.J., "Load Forecasting using Support Vector Machines: A Study on EUNITE Competition 2001", *Technical report, Department of Computer Science and Information Engineering, National Taiwan University*, 2002.
- [8] Guarnaccia C., Quartieri J., Tepedino C., Rodrigues E. R., "An analysis of airport noise data using a non-homogeneous Poisson model with a change-point", *Applied Acoustics*, Vol. 91, 2015, pp. 33-39.
- [9] Charytoniuk W., Chen M.S., Van Olinda P., "Nonparametric Regression Based Short-Term Load Forecasting", *IEEE Transactions on Power Systems*, 13 (1998) 725-730.
- [10] Morano, P., Tajani, F., "Least median of squares regression and minimum volume ellipsoid estimator for outliers detection in housing appraisal", *International Journal of Business Intelligence and Data Mining*, Vol. 9, No. 2, (2014), pp. 91-111.
- [11] Cho M.Y., Hwang J.C., and Chen C.S., "Customer Short-Term Load Forecasting by using ARIMA Transfer Function Model", *Proc. of the Int. Conf. on Energy Management and Power Delivery*, 1995, 1 pp. 317-322.
- [12] Feinberg E.A., Hajagos J.T., and Genethliou D., "Statistical Load Modeling", *Proc. of the 7th IASTED Int. Multi-Conf.: Power and Energy Systems*, Palm Springs, CA, 2003, pp. 88-91.
- [13] Kirtzis S.J. and Bakirtzis A.G., "A Fuzzy Expert System for Peak Load Forecasting: Application to the Greek Power System", *Proc. of the 10th Mediterranean Electrotechnical Conf.*, 2000, 3 pp. 1097-1100.
- [14] Quartieri J., Mastorakis N.E., Iannone G., Guarnaccia C., "A Cellular Automata Model for Fire Spreading Prediction", in *Latest Trends on Urban Planning and Transportation*, *Proc. of the 3rd Int. Conf. on "Urban Planning and Transportation"* (UPT '10), Corfu, Greece, 22-24 July 2010. ISBN: 978-960-474-204-2/ISSN: 1792-4286, pp. 173-179.
- [15] Iannone G., Troisi A., Guarnaccia C., D'Agostino P. P., Quartieri J., "An Urban Growth Model Based on a Cellular Automata Phenomenological Framework", *Int. Journal of Modern Physics C*, Volume 22, Issue 05, pp. 543-561. DOI: 10.1142/S0129183111016427, (2011).
- [16] Guarnaccia C., Quartieri J., Mastorakis N.E., Tepedino C., "Development and Application of a Time Series Predictive Model to Acoustical Noise Levels", *WSEAS Transactions on Systems*, Vol. 13, (2014) pp. 745-756, ISSN / E-ISSN: 1109-2777 / 2224-2678.
- [17] Guarnaccia C., Quartieri J., Rodrigues E.R., Tepedino C., "Acoustical Noise Analysis and Prediction by means of Multiple Seasonality Time Series Model", *International Journal of Mathematical Models and Methods in Applied Sciences*, Vol. 8, (2014) pp 384-393, ISSN: 1998-0140.
- [18] Guarnaccia C., Quartieri J., Barrios J.M., Rodrigues E.R., "Modelling Environmental Noise Exceedances Using non-Homogenous Poisson

- Processes”, *Journal of the Acoustical Society of America*, 136, (2014) pp. 1631-1639; <http://dx.doi.org/10.1121/1.4895662>
- [19] Guarnaccia C., “Advanced Tools for Traffic Noise Modelling and Prediction”, *WSEAS Transactions on Systems*, Issue 2, Vol.12, (2013) pp. 121-130.
- [20] Quartieri J., Mastorakis N.E., Iannone G., Guarnaccia C., D’Ambrosio S., Troisi A., Lenza T.L.L., “A Review of Traffic Noise Predictive Models”, *Proc. of the 5th WSEAS Int. Conf. on “Applied and Theoretical Mechanics” (MECHANICS’09)*, Puerto de la Cruz, Tenerife, Spain, December 14-16 2009, pp. 72-80.
- [21] Guarnaccia C., Lenza T.L.L., Mastorakis N.E., Quartieri J., “A Comparison between Traffic Noise Experimental Data and Predictive Models Results”, *International Journal of Mechanics*, Issue 4, Vol. 5, (2011) pp. 379-386, ISSN: 1998-4448.
- [22] Guarnaccia C., “Analysis of Traffic Noise in a Road Intersection Configuration”, *WSEAS Transactions on Systems*, Issue 8, Volume 9, (2010), pp.865-874, ISSN: 1109-2777.
- [23] Iannone G., Guarnaccia C., Quartieri J., “Speed Distribution Influence in Road Traffic Noise Prediction”, *Environmental Engineering And Management Journal*, Vol. 12, Issue 3, (2013) pp. 493-501.
- [24] Quartieri J., Iannone G., Guarnaccia C., “On the Improvement of Statistical Traffic Noise Prediction Tools”, *Proc. of the 11th WSEAS Int. Conf. on “Acoustics & Music: Theory & Applications” (AMTA '10)*, Iasi, Romania, June 13-15 2010, pp. 201-207.
- [25] Quartieri J., Mastorakis N.E., Guarnaccia C., Troisi A., D’Ambrosio S., Iannone G., “Traffic Noise Impact in Road Intersections”, *Int. Journal of Energy and Environment*, Issue 1, Volume 4 (2010), pp. 1-8.
- [26] Iannone G., Guarnaccia C., Quartieri J., “Noise Fundamental Diagram deduced by Traffic Dynamics”, in *Recent Researches in Geography, Geology, Energy, Environment and Biomedicine*, Proc. of the 4th WSEAS Int. Conf. on Engineering Mechanics, Structures, Engineering Geology (EMESEG '11), Corfù Island, Greece, July 14-16 2011, pp. 501-507.
- [27] Quartieri J., Mastorakis N.E., Guarnaccia C., Iannone G., “Cellular Automata Application to Traffic Noise Control”, *Proc. of the 12th Int. Conf. on “Automatic Control, Modelling & Simulation” (ACMOS '10)*, Catania (Italy), May 29-31 2010, pp. 299-304.
- [28] Guarnaccia C., “Acoustical Noise Analysis in Road Intersections: a Case Study”, *Proc. of the 11th WSEAS Int. Conf. on “Acoustics & Music: Theory & Applications” (AMTA '10)*, Iasi, Romania, June 13-15 2010, pp. 208-215.
- [29] Guarnaccia C., “New Perspectives in Road Traffic Noise Prediction”, in *Latest advances in Acoustics and Music*, *Proc. of the 13th Int. Conf. on Acoustics & Music: Theory & Applications (AMTA '12)*, Iasi, Romania, June 13-15 2012, pp. 255-260.
- [30] Quartieri J., Mastorakis N.E., Guarnaccia C., Troisi A., D’Ambrosio S., Iannone G., “Road Intersections Noise Impact on Urban Environment Quality”, *Proc. of the 5th WSEAS International Conference on “Applied and Theoretical Mechanics” (MECHANICS '09)*, Puerto de la Cruz, Tenerife, Spain, December 14-16 2009, pp. 162-171.
- [31] Guarnaccia C., Cerón Bretón J.G., Quartieri J., Tepedino C., Cerón Bretón R.M., “An Application of Time Series Analysis for Forecasting and Control of Carbon Monoxide Concentrations”, *International Journal of Mathematical Models and Methods in Applied Sciences*, Vol. 8, (2014) pp 505-515, ISSN: 1998-0140.
- [32] Pope C.A., Dockery D.W., Spengler J.D., and Raizenne M.E., “Respiratory Health and PM10 Pollution: A Daily Time Series Analysis”, *American Review of Respiratory Disease*, Vol. 144, No. 3\_pt\_1, (1991) pp. 668-674.
- [33] Dominici F., McDermott A., Zeger S.L., and Samet J.M., “On the Use of Generalized Additive Models in Time-Series Studies of Air Pollution and Health”, *American Journal of Epidemiology*, 156 (3), (2002) pp 193-203.
- [34] Di Matteo T., Aste T., Dacorogna M.M., “Scaling behaviors in differently developed markets”, *Physica A: Statistical Mechanics and its Applications*, Vol. 324, Issues 1–2, (2003) pp. 183-188.
- [35] Milanato D., *Demand Planning. Processi, metodologie e modelli matematici per la gestione della domanda commerciale*, Springer, Milano, 2008, in Italian.
- [36] Chase R.B., Aquilano N.J., *Operations Management for Competitive Advantage*, Irwin Professional Pub, 10th edition, 2004.
- [37] Ljung G.M., Box G.E.P., “On a measure of lack of fit in time series models”, *Biometrika*, 65, (1978) 297-303.
- [38] Box G.E.P., Pierce D.A., “Distribution of Residual Autocorrelations in Autoregressive-Integrated Moving Average Time Series Models”, *Journal of the American Statistical Association*, 65, (1970) 1509–1526.
- [39] Brockwell P.J., Davis R.A., *Introduction to Time Series and Forecasting*, Second Edition, Springer, 2002.
- [40] Lee T.H., White H., and Granger C.W.J., “Testing for neglected nonlinearity in time series models”, *Journal of Econometrics* 56, (1993) 269-290.
- [41] Teraesvirta T., Lin C.F., and Granger C.W.J., “Power of the Neural Network Linearity Test”, *Journal of Time Series Analysis*, 14 (1993) 209-220.
- [42] Said S.E. and Dickey D.A., “Testing for Unit Roots in Autoregressive-Moving Average Models of Unknown Order”. *Biometrika*, 71 (1984) 599-607.
- [43] Phillips P.C.B., Perron P., “Testing for a Unit Root in Time Series Regression”, *Biometrika* 75 (2), (1988) 335–346. doi:10.1093/biomet/75.2.335
- [44] <http://www.elektrotransportsf.com/index.php?lang=en> (November 2014)
- [45] Quartieri J., Troisi A., Guarnaccia C., Lenza TLL, D’Agostino P., D’Ambrosio S., Iannone G., “An Acoustical Study of High Speed Train Transits”, *WSEAS Transactions on Systems*, Issue 4, Vol.8, pp. 481-490 (2009).
- [46] Quartieri J., Troisi A., Guarnaccia C., Lenza TLL, D’Agostino P., D’Ambrosio S., Iannone G., “Application of a Predictive Acoustical Software for Modelling Low Speed Train Noise in an Urban Environment”, *WSEAS Transactions on Systems*, Issue 6, Vol.8, pp. 673-682 (2009).
- [47] Guarnaccia C., Mastorakis N.E., Quartieri J., “Wind Turbine Noise: Theoretical and Experimental Study”, *International Journal of Mechanics*, Issue 3, Vol.5, pp. 129-137 (2011).
- [48] Guarnaccia C., Mastorakis N. E., Quartieri J., “A Mathematical Approach for Wind Turbine Noise Propagation”, in *Applications of Mathematics and Computer Engineering, American Conference of Applied Mathematics (AMERICAN-MATH '11)*, Puerto Morelos, Mexico, 29-31 January 2011, pp. 187-194.
- [49] Guarnaccia C., Quartieri J., Mastorakis N. E. and Tepedino C., “Acoustic Noise Levels Predictive Model Based on Time Series Analysis”, in *Latest Trends in Circuits, Systems, Signal Processing and Automatic Control*, *proceedings of the 2nd Int. Conf. on Acoustics, Speech and Audio Processing (ASAP '14)*, Salerno, Italy, June 3-5, 2014, ISSN: 1790-5117, ISBN: 978-960-474-374-2, pp. 140-147.
- [50] Guarnaccia C., Quartieri J., Rodrigues E. R. and Tepedino C., “Time Series Model Application to Multiple Seasonality Acoustical Noise Levels Data Set”, in *Latest Trends in Circuits, Systems, Signal Processing and Automatic Control*, *proceedings of the 2nd Int. Conf. on Acoustics, Speech and Audio Processing (ASAP '14)*, Salerno, Italy, June 3-5, 2014, ISSN: 1790-5117, ISBN: 978-960-474-374-2, pp. 171-180.
- [51] Guarnaccia C., Quartieri J., Cerón Bretón J. G., Tepedino C., Cerón Bretón R. M., “Time Series Predictive Model Application to Air Pollution Assessment”, in *Latest Trends in Systems*, *Proc. of the 18th Int. Conf. on Circuits, Systems, Communications and Computers (CSCC'14)*, Santorini, Greece, 17-21 July 2014, pp. 499-505.